Nucleon pair approximation description of the low-lying structure of ^{108,109}Te and ^{109}I

H. Jiang,[1,2,3,*] C. Qi,[2,†] Y. Lei,[4] R. Liotta,[2] R. Wyss,[2] and Y. M. Zhao[3,5,‡]

[1]*School of Arts and Sciences, Shanghai Maritime University, Shanghai 201306, China*
[2]*Department of Physics, Royal Institute of Technology (KTH), SE-10691 Stockholm, Sweden*
[3]*Department of Physics and Shanghai Key Laboratory of Particle Physics and Cosmology, Shanghai Jiao Tong University, Shanghai 200240, China*
[4]*Key Laboratory of Neutron Physics, Institute of Nuclear Physics and Chemistry, China Academy of Engineering Physics, Mianyang 621900, China*
[5]*Center of Theoretical Nuclear Physics, National Laboratory of Heavy Ion Accelerator, Lanzhou 730000, China*

(Received 9 July 2013; revised manuscript received 25 September 2013; published 30 October 2013)

The low-lying level schemes and electromagnetic transitions of ^{109}Te, ^{109}I, and the neighboring even-even nucleus ^{108}Te are calculated within the framework of the SD-pair approximation of the nuclear shell model. Good agreement is obtained between the calculated results and experimental data. The favored components of low-lying bands are discussed in the collective nucleon-pair subspace. The weak-coupling picture shown in these nuclei and its relationship with residual quadrupole-quadrupole interaction between valence protons and neutrons are analyzed.

DOI: 10.1103/PhysRevC.88.044332 PACS number(s): 21.10.Re, 21.10.Pc, 21.60.Ev, 23.20.Lv

I. INTRODUCTION

Great experimental and theoretical efforts have been made in recent years to study the structure and decay properties of neutron-deficient tin, tellurium, iodine, and xenon isotopes near the $N = Z = 50$ closed shells [1–12]. Towards the proton drip line, these nuclei become unstable against particle emissions [13–16]. α decays have been observed in nuclei $^{105-110}$Te and $^{108-113}$I [1,13], and the nucleus ^{109}I is known as a proton emitter [14,16]. Another feature of particular interest in this mass region is the behavior of the band structure and electromagnetic transition properties in relation to the doubly magic nucleus ^{100}Sn. The spectroscopic studies suggest a vibrational-like collective character in even-even tellurium nuclei [17,18]. The manifestation of vibrational collectivity in these nuclei is, however, not supported by $B(E2)$ measurements [19]. Octupole correlations were found in the nuclei ^{108,109}Te [20,21]. Bands built on the $\nu h_{11/2}$ and $\pi h_{11/2}$ orbits are systematically observed in the odd-mass tellurium and iodine isotopes. The low-lying $\nu h_{11/2}$ bands in odd-mass tellurium isotopes follow the same trend as those yrast states in the even-even core [4,22–24]. This was explained in terms of core-particle coupling [22]. The $\pi h_{11/2}$ bands for odd-mass iodine isotopes reflect a decrease in quadrupole deformation moving away from the midshell, with the maximum occurring in ^{117,119}I [25].

The measurement of electromagnetic transitions in this nuclear region is a challenging task due to the very small reaction cross sections leading to the nuclei of interest. So far, the lightest tin, tellurium, and iodine nuclei with known reduced transition probabilities are ^{104}Sn [2], ^{108}Te [3], ^{109}Te [4], and ^{109}I [5]. Few theoretical studies have been carried out to analyze the band structures and electromagnetic transitions in the nuclei ^{109}Te and ^{109}I. Among these works, cranked Woods-Saxon calculations [25] interpreted the band structures of ^{109}I as being built on the $\pi g_{7/2}$ and $\pi h_{11/2}$ states in a weakly triaxial deformed nucleus. Interacting boson-fermion model calculations [26] discussed the band structures of ^{109}Te and identified two favored bands built on the $\nu g_{7/2}$ and $\nu h_{11/2}$ neutron quasiparticle states. Shell-model calculations with the realistic charge-dependent Bonn nucleon-nucleon potential on ^{109}Te [4] and ^{109}I [5] reproduced the experimental excitation energies but showed large deviations from the experimental $B(E2)$ strengths in certain cases.

Recent lifetime measurements on ^{108}Te [3], ^{109}Te [4], and ^{109}I [5] showed that the $B(E2)$ values are approximately equal. This suggests that the additional proton (or neutron) in ^{109}I (or ^{109}Te) might have negligible effect on the reduced transition probabilities. Based on shell-model calculations, it was speculated that in these states the additional unpaired nucleon is weakly coupled to the even-even core ^{108}Te [4,5].

The purpose of this paper is to study the low-lying band structures and electromagnetic transitions in the nuclei ^{108,109}Te and ^{109}I within the framework of the nucleon pair approximation (NPA). The NPA [27] has been shown to be a reliable and economic approximation of the shell model. It has been successfully applied to describe even-even, odd-A, and odd-odd nuclei with $A \sim 80$ [28], 100 [9], 130 [29], and 210 [30]. In this model, the dimension of the collective nucleon-pair subspace is small, thus providing a simple and illuminating picture of the structure of the nuclei under investigation. In particular it allows one to evaluate the probability of the existence of weak-coupling schemes in a straightforward manner.

This paper is organized as follows. In Sec. II we give a brief introduction to the nucleon pair approximation, including the basis, the Hamiltonian, the transition operators, and the parametrization of our calculations. In Sec. III we present our calculations on the excitation energies of the low-lying

*huijiang@shmtu.edu.cn
†chongq@kth.se
‡Corresponding author: ymzhao@sjtu.edu.cn

states, their dominant configurations, and the electromagnetic transition properties. Our summary and conclusion are given in Sec. IV.

II. THEORETICAL FRAMEWORK

For medium-heavy nuclei, the dimension of the shell-model configuration space is usually prohibitively large and one must resort to various truncation schemes, e.g., the interacting boson model [31], the broken pair approximation [32], the fermion dynamical symmetry model [33] as well as the NPA [27]. In the NPA approach, a collective pair with angular momentum r and projection M is defined as [27]

$$A^{(r)\dagger}_{M\sigma} = \sum_{j_\sigma j'_\sigma} y(j_\sigma j'_\sigma r)\big(C^\dagger_{j_\sigma} \times C^\dagger_{j'_\sigma}\big)^{(r)}_M,$$

where $C^\dagger_{j_\sigma}$ is the single-particle creation operator in the j orbit, and $\sigma = \pi$ and ν are the index of proton and neutron degrees of freedom, respectively. $r = 0, 2, 4, 6, 8$ corresponds to S, D, G, I, and K pairs. The numbers $y(j_\sigma j'_\sigma r)$ are the so-called structure coefficients of the nucleon pair with spin r.

In an even-even system with $2N$ valence protons or neutrons, we assume that all the valence nucleons are coupled to collective pairs. Our collective nuclear pair subspace is constructed by coupling N collective pairs $r_1, r_2, \ldots, r_N$ stepwise,

$$A^{(J_N)\dagger}_{M_{J_N}}(r_1 r_2 \cdots r_N, J_1 J_2 \cdots J_N)|0\rangle \equiv A^{(J_N)\dagger}_{M_{J_N}}|0\rangle = [\cdots (A^{r_1\dagger} \times A^{r_2\dagger})^{(J_2)} \times \cdots \times A^{r_N\dagger}]^{(J_N)}_{M_{J_N}}|0\rangle.$$

Similarly, for an odd-A system with $2N+1$ valence protons or neutrons, all valence nucleons are paired except the last nucleon, which can occupy any single-particle level j of the shell-model space under consideration. Our nucleon-pair subspace is given by successively coupling the N nucleon pairs to the unpaired nucleon in a single-j orbit as

$$A^{(J_N)\dagger}_{M_{J_N}}(j r_1 r_2 \cdots r_N, J_1 J_2 \cdots J_N)|0\rangle \equiv A^{(J_N)\dagger}_{M_{J_N}}|0\rangle = \{\cdots [(C^\dagger_j \times A^{r_1\dagger})^{(J_1)} \times A^{r_2\dagger}]^{(J_2)} \times \cdots \times A^{r_N\dagger}\}^{(J_N)}_{M_{J_N}}|0\rangle,$$

where J_i (half integer) denotes the total angular momentum for the first $2i+1$ nucleons.

As in Ref. [27], we choose in our calculations a complete set of non-orthonormal but linearly independent many-pair basis states. If the basis states are chosen appropriately, all the eigenvalues of the overlap matrix $\langle 0|A^{(J'_N)}_{M_{J'_N}} A^{(J_N)\dagger}_{M_{J_N}}|0\rangle$ are non-zero. This practice guarantees that all multi-pair basis states in the NPA calculations are not over-complete.

The NPA Hamiltonian is chosen to have the form

$$H = \sum_{j_\sigma} \epsilon_{j_\sigma} C^\dagger_{j_\sigma} C_{j_\sigma} + \sum_\sigma \big(G^0_\sigma \mathcal{P}^{(0)\dagger}_\sigma \cdot \mathcal{P}^{(0)}_\sigma + G^2_\sigma \mathcal{P}^{(2)\dagger}_\sigma \cdot \mathcal{P}^{(2)}_\sigma\big) + \sum_\sigma \kappa_\sigma Q_\sigma \cdot Q_\sigma + \kappa_{\pi\nu} Q_\pi \cdot Q_\nu, \quad (1)$$

where ϵ_{j_σ} is the single-particle energy, G^0_σ, G^2_σ, κ_σ, and $\kappa_{\pi\nu}$ are the two-body interaction strengths corresponding to monopole, quadrupole pairing, and quadrupole-quadrupole interactions between valence nucleons. We have

$$\mathcal{P}^{(0)\dagger}_\sigma = \sum_{j_\sigma} \frac{\sqrt{2j_\sigma+1}}{2}\big(C^\dagger_{j_\sigma} \times C^\dagger_{j_\sigma}\big)^{(0)}_0,$$

$$\mathcal{P}^{(2)\dagger}_\sigma = \sum_{j_\sigma j'_\sigma} q(j_\sigma j'_\sigma)\big(C^\dagger_{j_\sigma} \times C^\dagger_{j'_\sigma}\big)^{(2)}_M,$$

$$Q_\sigma = \sum_{j_\sigma j'_\sigma} q(j_\sigma j'_\sigma)\big(C^\dagger_{j_\sigma} \times \tilde{C}_{j'_\sigma}\big)^{(2)}_M,$$

where $q(jj') = \frac{(-)^{j-1/2}}{\sqrt{20\pi}} \hat{j}\hat{j}' C^{20}_{j1/2,j'-1/2}\langle nl|r^2|nl'\rangle$. $C^{20}_{j1/2,j'-1/2}$ is the Clebsch-Gordan coefficient. The isospin symmetry is not conserved in our NPA Hamiltonian. But it has to be pointed out that the effect of isospin mixture on the low-lying states

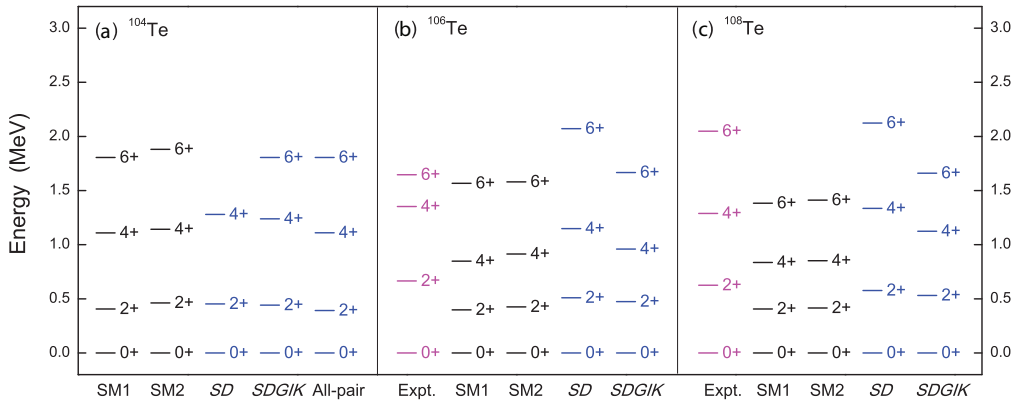

FIG. 1. (Color online) Ground state bands in (a) ^{104}Te, (b) ^{106}Te, and (c) ^{108}Te. The experimental data are taken from Ref. [17]. The shell-model calculations without isospin symmetry (denoted by SM1), the SD-pair approximation (denoted by SD), the $SDGIK$-pair approximation (denoted by $SDGIK$), and the calculations in the subspace constructed by all possible NPA pairs (denoted by All-pair) are performed with the same phenomenological interactions in Eq. (1). The shell-model calculations with isospin symmetry (denoted by SM2) are shown for comparison.

TABLE I. Single-particle (s.p.) energies ϵ_{j_σ} (in MeV) and two-body interaction parameters G^0_σ, G^2_σ, κ_σ, $\kappa_{\pi\nu}$. The unit of G^0_σ is MeV; the units of G^2_σ, κ_σ, and $\kappa_{\pi\nu}$ are MeV/r_0^4, $r_0^2 = 1.012A^{1/3}$ fm^2. $\sigma = \pi, \nu$ stand for proton and neutron, respectively.

j	$s_{1/2}$	$d_{3/2}$	$d_{5/2}$	$g_{7/2}$	$h_{11/2}$	
ϵ_{j_π}	1.550	1.660	0.172	0.000	3.550	
ϵ_{j_ν}	1.550	1.660	0.172	0.000	3.550	
G^0_ν	G^2_ν	κ_ν	G^0_π	G^2_π	κ_π	$\kappa_{\pi\nu}$
−0.18	−0.036	−0.015	−0.20	−0.036	−0.0125	−0.05

is small for the nuclei treated here. To illustrate this point, we compare the ground state bands for ^{104,106,108}Te between the shell-model calculations without (denoted by SM1) and with isospin symmetry (denoted by SM2) in Fig. 1. It is seen that both calculations give rather similar results.

The single-particle energies and two-body interaction parameters in our calculations are shown in Table I. The neutron single-particle energies of $g_{7/2}$ and $d_{5/2}$ orbitals are taken from the experimental excitation energies in ^{101}Sn [8]. There are no experimental data for the remaining orbitals. Their single-particle energies are extracted from a shell-model calculation [34]. The proton single-particle energies are taken to be the same as those for neutrons.

There are a total of seven parameters for the two-body interactions: G^0_π, G^0_ν, G^2_π, G^2_ν, κ_π, κ_ν, and $\kappa_{\pi\nu}$. For ^{109}Te and ^{109}I, we assume the same parameters as for their even-even core ^{108}Te. We take $G^0_\nu = -0.18$ MeV, which is the same value as the one used in Ref. [9]. Because the proton number is close to the neutron number in this region, we adopt for the strength of the proton interaction the value $G^0_\pi = -0.20$ MeV. The remaining five parameters are obtained by fitting to the excitation energies and $B(E2)$ values in nuclei ^{108,109}Te and ^{109}I.

The $E2$ transition operator is defined by $T(E2) = e_\pi Q_\pi + e_\nu Q_\nu$, where e_π and e_ν are the effective charges of valence protons and neutrons, respectively. The $B(E2)$ value in units of e^2 fm^4 is given by

$$B(E2, J_i \to J_f) = \frac{2J_f + 1}{2J_i + 1}(e_\pi \chi_\pi + e_\nu \chi_\nu)^2 r_0^4, \qquad (2)$$

with reduced matrix element $\chi_\sigma = \langle \beta_f, J_f || Q_\sigma || \beta_i, J_i \rangle$ $(\sigma = \pi, \nu)$ and $r_0^2 = 1.012A^{1/3}$ fm^2. $|\beta_i, J_i\rangle$ is the eigenfunction of the J_i state. Our neutron effective charge is taken to be $e_\nu = 1.28e$, the same as for tin isotopes [9]. The proton effective charge $e_\pi = 1.79e$ is obtained by fitting to experimental data.

The $M1$ transition operator is defined by $T(M1) = g_{l\pi} l_\pi + g_{l\nu} l_\nu + g_{s\pi} s_\pi + g_{s\nu} s_\nu$, where l_σ and s_σ are the orbital and spin angular momenta, and $g_{l\sigma}$ and $g_{s\sigma}$ are the effective orbital and spin gyromagnetic ratios, respectively. The effective spin gyromagnetic ratios are taken to be $g_{s\pi} = 5.586 \times 0.7\mu_N$ and $g_{s\nu} = -3.826 \times 0.7\mu_N$, where the number 0.7 is the conventional quenching factor (see also Ref. [10]). Two sets of effective orbital gyromagnetic ratios are used in this paper. In the first set, we use their free values, i.e., $g_{l\nu} = 0\mu_N$ and $g_{l\pi} = 1\mu_N$. In the other set, we take $g_{l\nu} = 0\mu_N$ and $g_{l\pi} = 1.35\mu_N$, which are the optimized parameters determined by fitting to the experimental data in this region.

Our nucleon pair subspace is constructed by SD pairs of valence protons and neutrons, with respect to the doubly closed shell nucleus ^{100}Sn. We have also investigated the $SDGIK$-pair subspace and found that the G, I, K pairs do not contribute significantly to the low-lying states of the nuclei ^{108,109}Te and ^{109}I. As in Ref. [29], we use the BCS pairs as our S pair. The D pair is obtained by using the commutator $D^\dagger = \frac{1}{2}[Q, S^\dagger]$ [32].

It was shown in Ref. [35] that the NPA is an efficient truncation scheme of the shell model for nuclei ^{44,46}Ca, ^{130,131}Te, and ^{132}I by using phenomenological as well as realistic interactions. In order to probe the validity of the NPA for the nuclei to be studied here we also performed the shell model as well as the NPA calculations and compared the results. In Fig. 1, we make comparisons of ground state bands for ^{104}Te, ^{106}Te, and ^{108}Te calculated by SD-pair approximation (denoted by SD), $SDGIK$-pair approximation (denoted by

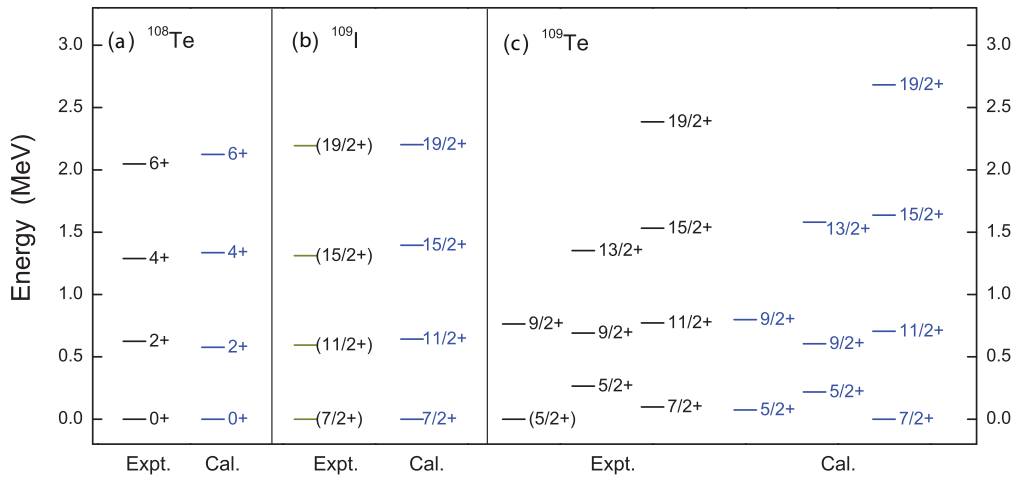

FIG. 2. (Color online) Partial level schemes for low-lying positive-parity states in (a) ^{108}Te, (b) ^{109}I, and (c) ^{109}Te. The experimental data of ^{108,109}Te and ^{109}I are taken from Refs. [17] and [25], respectively.

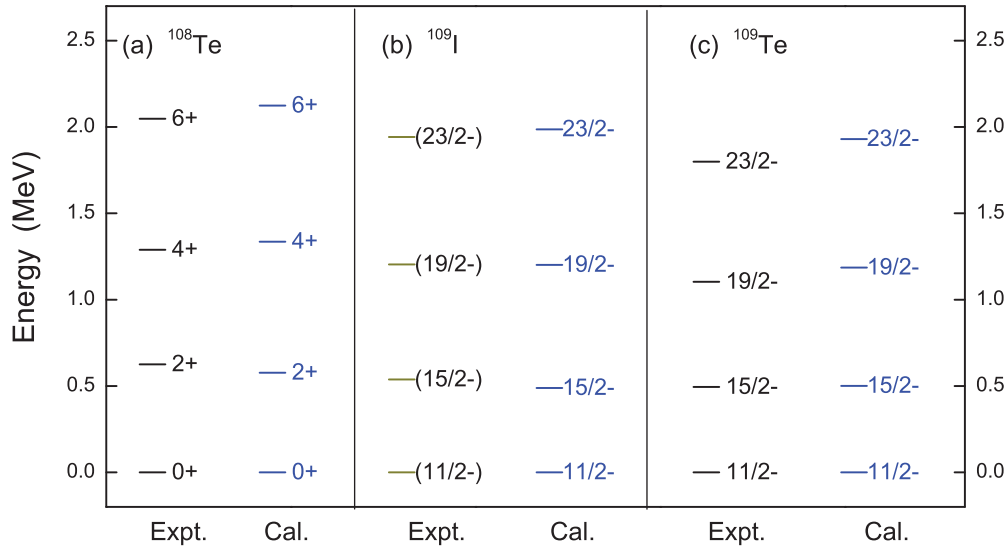

FIG. 3. (Color online) Same as Fig. 2 but for low-lying $h_{11/2}$ bands of ^{109}I and ^{109}Te in comparison with the ground state band in ^{108}Te, plotted relative to the bandheads.

$SDGIK$), the calculation in the subspace constructed by all possible NPA pairs (denoted by All-pair) and the shell model (denoted by SM1) by taking the same phenomenological interactions in Eq. (1). It is shown that the results of the SD reasonably agree with those of the SM1 (especially for the 2_1^+ state), indicating that the SD pairs are very important in building up low-lying states. For the nucleus ^{108}Te, our SD NPA calculation noticeably overestimates the excitation energy of the yrast 6^+ state in comparison with that of the shell model, due to the influence of other pairs, namely, G, I, K. If all possible NPA pairs are taken into account [see Fig. 1(a) for ^{104}Te], our results are equivalent to those of the SM1. Moreover, it is to be pointed out that the remarkable feature in Figs. 2 and 3 is that the SD-pair approximation agrees well with the experiment. This indicates that the SD-pair approximation with the phenomenological interactions is very well fitted to explain low-lying states in these nearly spherical nuclei, especially the energies and $E2$ transition properties of the 2_1^+ state of concern (see Fig. 4, Tables II and III). A much more sophisticated treatment of the effective interaction may be necessary for calculations in a larger space with more pairs or within the shell-model framework in order to get a better agreement with experimental data.

III. CALCULATIONS AND DISCUSSIONS

Our calculated low-lying energy levels and electromagnetic transitions are presented in Figs. 2–4 and Tables II–IV. The experimental excitation energies of nuclei ^{108,109}Te and ^{109}I are taken from Refs. [17,25]. The experimental electromagnetic transitions are taken from ^{108}Te [3], ^{109}Te [4], and ^{109}I [5]. The experimental $B(E2, 9/2_1^+ \rightarrow 5/2_1^+)$ measurement in ^{109}Te is not available at present. We present their theoretical values in Fig. 4 for comparison. The shell-model results (SM) are from Refs. [4,5].

One sees in Figs. 2 and 3 that our calculated energies reproduce reasonably well the corresponding experimental values. The relative level schemes of some states in ^{108}Te and ^{109}I are close to each other, suggesting that the additional proton in ^{109}I might be weakly coupled to the even-even core ^{108}Te [5]. That is, an unpaired proton in a single-j orbit (πj) might be coupled to the λ state of ^{108}Te [$|^{108}\mathrm{Te}(\lambda)\rangle$] to induce the k state of ^{109}I, i.e., $|^{109}\mathrm{I}(k)\rangle = |(\pi j)\otimes{}^{108}\mathrm{Te}(\lambda); k\rangle$. The nucleus ^{109}Te shows a similar pattern.

To understand the structures of these states we analyze them within our collective nucleon pair subspace. As discussed above, the resulting NPA wave function for the k state, i.e.,

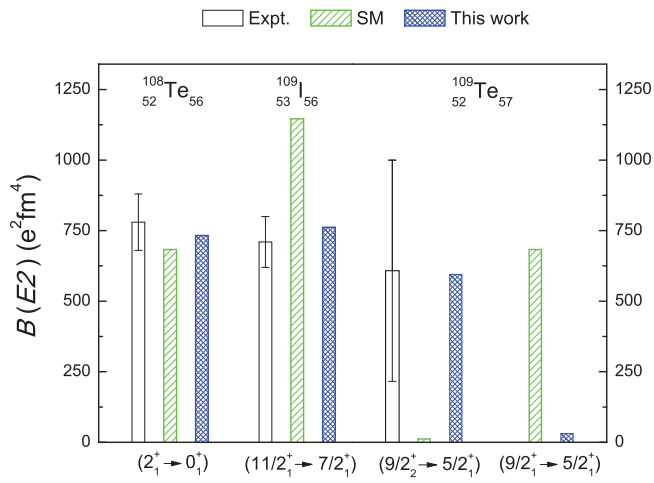

FIG. 4. (Color online) Comparison between theoretical $B(E2)$ transitions and the experimental data for nuclei ^{108}Te [3], ^{109}I [5], and ^{109}Te [4]. The shell-model results (SM) are taken from Refs. [4,5]. One sees the experimental ground state transitions between ^{108}Te, ^{109}I, and ^{109}Te are approximately equal, which indicates that the extra proton (or neutron) in ^{109}I (or ^{109}Te) has no significant effect on the reduced transition probabilities for these states.

TABLE II. The $B(E2, J_i \to J_f)$ values in units of $e^2\text{fm}^4$. The columns χ_σ ($\sigma = \pi, \nu$) show the reduced matrix elements of Eq. (2). The experimental data and shell-model results are taken from [a]Ref. [3], [b]Ref. [5] and [c]Ref. [4].

	J_i	J_f	Expt.	NPA	SM	χ_π	χ_ν
^{108}Te							
	2_1^+	0_1^+	$780(^{+100}_{-80})^a$	733	680[c]	3.429	5.009
	4_1^+	2_1^+	–	894	–	1.633	4.215
^{109}I							
	$11/2_1^+$	$7/2_1^+$	710(90)[b]	762	1146[b]	1.757	3.003
	$15/2_1^+$	$11/2_1^+$	–	1034	–	1.625	3.724
	$15/2_1^-$	$11/2_1^-$	–	880	–	1.986	2.753
	$19/2_1^-$	$15/2_1^-$	–	983	–	1.473	3.603
^{109}Te							
	$9/2_2^+$	$5/2_1^+$	608(392)[c]	595	12[c]	2.096	2.153
	$9/2_1^+$	$5/2_1^+$	–	31	683[c]	0.443	0.550
	$9/2_1^+$	$5/2_2^+$	340(93)[c]	56	6[c]	0.585	0.737
	$9/2_2^+$	$5/2_2^+$	–	0.46	407[c]	−0.063	0.231
	$13/2_1^+$	$9/2_1^+$	–	310	850[c]	0.785	2.270
	$11/2_1^+$	$7/2_1^+$	–	583	810[c]	1.804	2.254
	$15/2_1^+$	$11/2_1^+$	–	719	–	1.420	3.016
	$15/2_1^-$	$11/2_1^-$	–	861	–	1.810	2.941
	$19/2_1^-$	$15/2_1^-$	–	1005	–	1.458	3.686

$|^{109}\text{I}(k)\rangle$ and $|^{109}\text{Te}(k)\rangle$, contains many components consisting of S and D pairs plus the unpaired nucleon which may occupy any single-j orbit in Table I. To evaluate the probability that a weakly coupled state is included in the NPA wave function, we evaluate the overlaps $\langle ^{109}\text{I}(k)|(\pi j) \otimes ^{108}\text{Te}(\lambda); k\rangle$ and $\langle ^{109}\text{Te}(k)|(\nu j) \otimes ^{108}\text{Te}(\lambda); k\rangle$. The results are given in Table V. One sees therein that for the states of interest, i.e., those in Figs. 2 and 3, the overlaps are indeed very large. This suggests that these states can be well represented by the weak coupling between a collective state in the even-even "core" and the unpaired nucleon in a single-j orbit. This is also a strong indication of the vibrational-like character of nuclei in this region, where the ground as well as low-lying excited states behave like boson degrees of freedom, practically unperturbed by the presence of the odd nucleon.

The states of ^{109}I shown in Figs. 2(b) and 3(b) are clearly seen to arise from the coupling of the vibrational-like ground state band in ^{108}Te with the unpaired proton in the $\pi g_{7/2}$ [Fig. 2(b)] and $\pi h_{11/2}$ [Fig. 3(b)] orbit. This is indeed confirmed by the large wave function overlap between the corresponding states in Table V.

The analysis of the positive-parity bands of ^{109}Te in Fig. 2(c) is more involved. In order to understand the relation between these states and their eventual (if any) weak coupling description, one needs to rely on the calculated overlaps of Table V. One sees that the states $5/2_1^+$ and $9/2_2^+$, forming the first band in Fig. 2(c), are built upon the coupling of the $\nu d_{5/2}$ orbit with the collective core states. Instead, the states $5/2_2^+$, $9/2_1^+$, and $13/2_1^+$, which form the second band in that figure, are atypical, because it arises from the coupling of the $\nu g_{7/2}$ orbit with only the 2_1^+ and 4_1^+ states in ^{108}Te. The third band is again a weak coupling band, because it arises as the coupling of the orbit $\nu g_{7/2}$ with all the states in ^{108}Te. The negative-parity band in Fig. 3(c) is also a typical weak coupling band, arising from the coupling of the $\nu h_{11/2}$ orbit with the core states. It is to be pointed out that our results largely agree with what was concluded in Refs. [25,26,36].

TABLE III. The $B(M1, J_i \to J_f)$ values of ^{109}Te in units of $10^{-3}\mu_N^2$. For the proton effective orbital gyromagnetic ratio, we adopt the value $g_{l\pi} = 1\mu_N$ in NPA-1 and $g_{l\pi} = 1.35\mu_N$ in NPA-2. The experimental data and shell-model results are from Ref. [4].

J_i	J_f	Expt.	NPA-1	NPA-2	SM
$7/2_1^+$	$5/2_1^+$	–	3	2	151
$7/2_1^+$	$5/2_2^+$	–	6	5	55
$7/2_2^+$	$5/2_1^+$	–	4	10	2
$7/2_2^+$	$5/2_2^+$	–	0.2	13	76
$9/2_1^+$	$7/2_1^+$	6(1)	1	10	162
$9/2_1^+$	$7/2_2^+$	–	24	150	126
$9/2_2^+$	$7/2_1^+$	–	16	15	0
$9/2_2^+$	$7/2_2^+$	137(92)	57	127	102

TABLE IV. Same as Table III except for magnetic moments μ (in units of μ_N) predicted in this work.

	NPA-1	NPA-2		NPA-1	NPA-2
^{108}Te			^{109}I		
2_1^+	+0.910	+1.237	$7/2_1^+$	+2.282	+3.592
4_1^+	+1.001	+1.331	$11/2_1^+$	+2.954	+4.510
^{109}Te					
$5/2_1^+$	−1.096	−1.078	$5/2_2^+$	+0.568	+0.593
$9/2_1^+$	+1.582	+1.888	$9/2_2^+$	+0.269	+0.737
$7/2_1^+$	+1.034	+1.051	$11/2_1^+$	+2.008	+2.395

TABLE V. Absolute values of overlaps between the calculated NPA low-lying states of ^{109}I (or ^{109}Te) and the corresponding weak-coupling wave function $|(\sigma j)\otimes^{108}\text{Te}(\lambda);k\rangle$. k and λ correspond to the state of the odd-mass nucleus and its neighboring even-even core ^{108}Te, respectively. σj ($\sigma=\pi,\nu$) refers to the unpaired valence nucleon in a single-j orbit.

^{109}I			^{109}Te		
$\|^{109}\text{I}(k)\rangle$	$\|(\pi j)\otimes^{108}\text{Te}(\lambda);k\rangle$	Overlap	$\|^{109}\text{Te}(k)\rangle$	$\|(\nu j)\otimes^{108}\text{Te}(\lambda);k\rangle$	Overlap
$\|7/2_1^+\rangle$	$\|(\pi g_{7/2})\otimes(0_1^+)\rangle$	0.82	$\|5/2_1^+\rangle$	$\|(\nu d_{5/2})\otimes(0_1^+)\rangle$	0.94
$\|11/2_1^+\rangle$	$\|(\pi g_{7/2})\otimes(2_1^+)\rangle$	0.86	$\|9/2_2^+\rangle$	$\|(\nu d_{5/2})\otimes(2_1^+)\rangle$	0.89
$\|15/2_1^+\rangle$	$\|(\pi g_{7/2})\otimes(4_1^+)\rangle$	0.87	$\|5/2_2^+\rangle$	$\|(\nu g_{7/2})\otimes(2_1^+)\rangle$	0.81
$\|19/2_1^+\rangle$	$\|(\pi g_{7/2})\otimes(6_1^+)\rangle$	0.93	$\|9/2_1^+\rangle$	$\|(\nu g_{7/2})\otimes(2_1^+)\rangle$	0.89
$\|11/2_1^-\rangle$	$\|(\pi h_{11/2})\otimes(0_1^+)\rangle$	0.85	$\|13/2_1^+\rangle$	$\|(\nu g_{7/2})\otimes(4_1^+)\rangle$	0.77
$\|15/2_1^-\rangle$	$\|(\pi h_{11/2})\otimes(2_1^+)\rangle$	0.91	$\|7/2_1^+\rangle$	$\|(\nu g_{7/2})\otimes(0_1^+)\rangle$	0.93
$\|19/2_1^-\rangle$	$\|(\pi h_{11/2})\otimes(4_1^+)\rangle$	0.92	$\|11/2_1^+\rangle$	$\|(\nu g_{7/2})\otimes(2_1^+)\rangle$	0.92
$\|23/2_1^-\rangle$	$\|(\pi h_{11/2})\otimes(6_1^+)\rangle$	0.95	$\|15/2_1^+\rangle$	$\|(\nu g_{7/2})\otimes(4_1^+)\rangle$	0.89
			$\|19/2_1^+\rangle$	$\|(\nu g_{7/2})\otimes(6_1^+)\rangle$	0.93
			$\|11/2_1^-\rangle$	$\|(\nu h_{11/2})\otimes(0_1^+)\rangle$	0.95
			$\|15/2_1^-\rangle$	$\|(\nu h_{11/2})\otimes(2_1^+)\rangle$	0.98
			$\|19/2_1^-\rangle$	$\|(\nu h_{11/2})\otimes(4_1^+)\rangle$	0.99
			$\|23/2_1^-\rangle$	$\|(\nu h_{11/2})\otimes(6_1^+)\rangle$	0.99

Electromagnetic transition is another sensitive probe of the calculated wave functions. Unfortunately the experimental observations in this mass region are still scarce and the corresponding errors are relatively large. This can be seen in Fig. 4 and Tables II and III, where the available experimental $B(E2)$ and $B(M1)$ values as well as a shell model and our own NPA calculations are shown. In Table II we also list our reduced matrix elements χ_σ ($\sigma=\pi,\nu$) [see Eq. (2)]. Our predicted magnetic dipole moments (μ) of some low-lying states are presented in Table IV.

One sees in Fig. 4 and Tables II and III that our results agree quite well with available experimental data except for the $B(E2, 9/2_1^+\rightarrow 5/2_2^+)$ value in ^{109}Te. To explore this further, one might need new experimental data in addition to the available ones at present.

As seen in Fig. 4, the experimental $B(E2)$ transitions in the nuclei ^{108}Te, ^{109}I, and ^{109}Te are approximately the same. This is consistent with our previous results on the structure of these states, because it indicates that the additional nucleon of ^{109}I (or ^{109}Te) is indeed weakly coupled to the even-even core for these states, as suggested in Refs. [4,5].

One also sees in Fig. 4 that the shell-model calculations reproduce well the $B(E2, 2_1^+\rightarrow 0_1^+)$ value in ^{108}Te, but overestimate the $B(E2, 11/2_1^+\rightarrow 7/2_1^+)$ value in ^{109}I, and fail to describe the $B(E2, 9/2_2^+\rightarrow 5/2_1^+)$ value in ^{109}Te. Moreover, in Table II one sees that the theoretical $B(E2, 9/2_2^+\rightarrow 5/2_1^+)$ value of the SM, i.e., 12 $e^2\,\text{fm}^4$, is much smaller than the corresponding experimental data, i.e., 608(392) $e^2\,\text{fm}^4$. As this experimental value practically coincides with the SM one for the transition $(9/2_1^+)\rightarrow(5/2_1^+)$ (683 $e^2\,\text{fm}^4$), in Ref. [4] it was suggested that the ordering of the first two calculated excited $9/2^+$ states in ^{109}Te are inverted. This is not the case in our present calculation.

It thus seems that, as pointed out in Ref. [4], the presence of the single decoupled valence proton affects the total measured $B(E2)$ strengths in a manner that is not currently well understood. To investigate this point further we perform several attempts, particularly to survey the sensitivity of the $B(E2)$ values upon the different terms of the interaction entering the theory. This is not a trivial task, because at the same time we require that all the other calculated physical quantities, which agreed well with available experimental data, should remain practically unchanged. We could do this very lengthy task because in our NPA truncated space the computing time needed to perform the calculations is relatively short. In this search we finally find that those requirements are fulfilled if one varies the residual proton-neutron quadrupole-quadrupole interaction ($\kappa_{\pi\nu}$) in a range from -0.01 to -0.11 MeV/r_0^4. Our results are shown in Fig. 5. There are two remarkable features in this figure. First, our calculation reproduces the available experimental data in all the nuclei analyzed here, i.e., ^{108}Te, ^{109}Te, and ^{109}I, by using a strength $\kappa_{\pi\nu}\sim -0.05$ MeV/r_0^4. Instead, the shell-model results [4,5], which agree with experiment only in the nucleus ^{108}Te, are reproduced by using $\kappa_{\pi\nu}\sim -0.09$ MeV/r_0^4. This suggests that, as speculated in Refs. [4,5], the quadrupole-quadrupole correlation in the realistic shell-model interaction might be too strong for nuclei in this region. It also indicates that $\kappa_{\pi\nu}$ for these three nuclei is not as strong as the values predicted by empirical formulas (see Appendix B in Ref. [37]), i.e., $\kappa_{\pi\nu}=-0.08\sim -0.10$ MeV/r_0^4. The second striking feature seen in Fig. 5 is that the $B(E2)$ values in ^{109}I and ^{109}Te are very sensitive to $\kappa_{\pi\nu}$. Thus, in Fig. 5(b) the transition $^{109}\text{I}(11/2_1^+\rightarrow 7/2_1^+)$ increases rapidly, from about 500 to more than 1200 $e^2\,\text{fm}^4$, in the range of the figure. Even more striking is what Fig. 5(c) shows for the transition $^{109}\text{Te}(9/2_2^+\rightarrow 5/2_1^+)$, for which the $B(E2)$ value first remains rather constant at about 600 $e^2\,\text{fm}^4$ to suddenly, at $\kappa_{\pi\nu}=-0.07$ MeV/r_0^4, decrease to reach a vanishing value at $\kappa_{\pi\nu}=-0.1$ MeV/r_0^4. Finally, in Fig. 5(d) the transition $^{109}\text{Te}(9/2_1^+\rightarrow 5/2_1^+)$ increases from zero to about 300 $e^2\,\text{fm}^4$ when $\kappa_{\pi\nu}$ decreases from -0.07 to -0.11 MeV/r_0^4. This may explain why in the previous shell-model

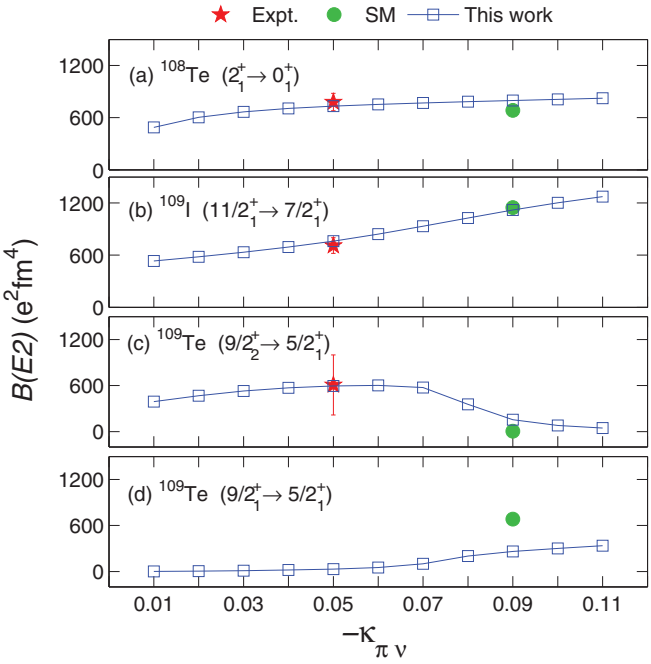

FIG. 5. (Color online) Same as Fig. 4 but for the theoretical $B(E2)$ values as a function of the quadrupole-quadrupole proton-neutron interaction strength $\kappa_{\pi\nu}$.

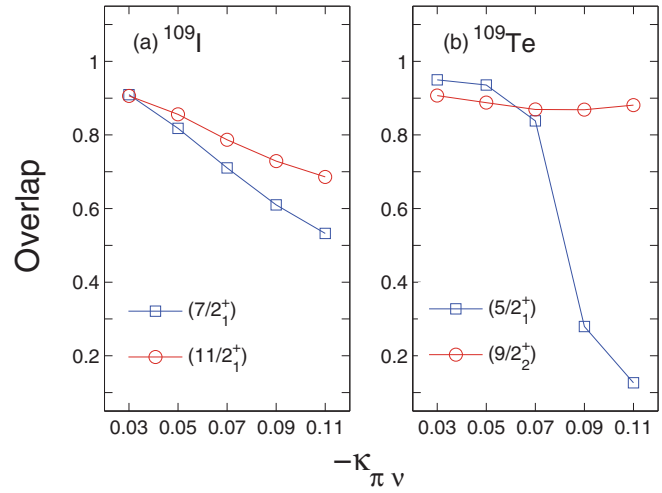

FIG. 6. (Color online) Absolute values of overlaps for some low-lying states vs $\kappa_{\pi\nu}$. (a) ^{109}I with $\langle ^{109}\mathrm{I}(7/2_1^+)|(\pi g_{7/2}) \otimes ^{108}\mathrm{Te}(0_1^+)\rangle$ and $\langle ^{109}\mathrm{I}(11/2_1^+)|(\pi g_{7/2}) \otimes ^{108}\mathrm{Te}(2_1^+)\rangle$, (b) ^{109}Te with $\langle ^{109}\mathrm{Te}(5/2_1^+)|(\nu d_{5/2}) \otimes ^{108}\mathrm{Te}(0_1^+)\rangle$ and $\langle ^{109}\mathrm{Te}(9/2_2^+)|(\nu d_{5/2}) \otimes ^{108}\mathrm{Te}(2_1^+)\rangle$.

calculation [4], the two $9/2^+ \rightarrow 5/2^+$ transitions are calculated to be inverted.

This behavior of the $B(E2)$ values in ^{109}Te, which follows a rather smooth curve as a function of the proton-neutron interaction strength, shows a deviation at $\kappa_{\pi\nu} \sim -0.07$ MeV/r_0^4 in Figs. 5(c) and 5(d). There is a peculiarity here, namely, that the state $^{109}\mathrm{Te}(5/2_1^+)$ is common in the transitions seen in those figures. We analyze the evolution of the structures of the states involved in those transitions as a function of $\kappa_{\pi\nu}$ and find that the dominant NPA configuration of the state $^{109}\mathrm{Te}(5/2_1^+)$ changes from $|(d_{5/2})_\nu S_\nu^3 S_\pi\rangle$ to $|(g_{7/2})_\nu D_\nu S_\nu^2 S_\pi\rangle$ when $\kappa_{\pi\nu}$ varies from -0.07 to -0.09 MeV/r_0^4. This change does not occur in the states $^{109}\mathrm{Te}(9/2_1^+)$ and $^{109}\mathrm{Te}(9/2_2^+)$.

We complete the analysis of the weak coupling wave functions by evaluating, as a function of $\kappa_{\pi\nu}$, their overlaps with the states $^{109}\mathrm{I}(7/2_1^+)$, $^{109}\mathrm{I}(11/2_1^+)$, $^{109}\mathrm{Te}(5/2_1^+)$, and $^{109}\mathrm{Te}(9/2_2^+)$. These overlaps are shown in Fig. 6. One sees that the overlaps of ^{109}I in Fig. 6(a) decrease with increasing $-\kappa_{\pi\nu}$, and the most rapid changes occur for the state $7/2_1^+$. Instead, the weak coupling description of the state $^{109}\mathrm{Te}(9/2_2^+)$ in Fig. 6(b), is practically independent of $\kappa_{\pi\nu}$. But the most striking feature in this figure is the very sharp change of the overlap corresponding to the state $5/2_1^+$ when $\kappa_{\pi\nu}$ varies from -0.07 to -0.09 MeV/r_0^4. As mentioned above, this abrupt change is a consequence of the evolution of the NPA wave function, which at that value (-0.09 MeV/r_0^4) of the strength the NPA configuration $|(g_{7/2})_\nu D_\nu S_\nu^2 S_\pi\rangle$ becomes dominant. This analysis shows that the value of the proton-neutron interaction strength $\kappa_{\pi\nu}$ is weak. Perhaps most important is that with the weak strength, the theoretical $B(E2, 11/2_1^+ \rightarrow 7/2_1^+)$ value in ^{109}I and $B(E2, 9/2_2^+ \rightarrow 5/2_1^+)$ value in ^{109}Te acquire the experimental value (within the experimental error) of 762 and 595 e^2 fm^4, as shown in Fig. 6 and Table II.

IV. SUMMARY

In this paper we have calculated the low-lying level schemes and electromagnetic transition properties of the nuclei ^{108}Te, ^{109}Te, and ^{109}I within the nucleon pair approximation (NPA) of the shell model. We extract from the NPA wave functions the probabilities that the low-lying bands in ^{109}I and ^{109}Te could be interpreted in terms of the weak coupling between the collective even-even core ^{108}Te and the unpaired particle. We thus find that that is indeed the case, as shown in Table V. This is consistent with the conjectures put forward in Refs. [4,5].

We probe the weak coupling pictures of the states by investigating the corresponding $B(E2)$ values and find that the calculated electromagnetic transitions to the ground states of ^{109}Te and ^{109}I are very sensitive to the residual quadrupole-quadrupole proton-neutron interaction $\kappa_{\pi\nu}$. By comparing with experimental data, we conclude that the proton-neutron interaction is weak and that the states $7/2_1^+$ and $11/2_1^+$ in ^{109}I as well as the states $5/2_1^+$ and $9/2_2^+$ in ^{109}Te are well described by the weak coupling scheme.

We tabulate our calculated $B(E2)$, $B(M1)$, and μ values for some low-lying states. Except for the transition $B(E2, 9/2_1^+ \rightarrow 5/2_2^+)$, our results agree very well with available experimental data, thus confirming the experimental order of the first two excited $9/2^+$ states in ^{109}Te.

The overall agreement between the calculations and experiments regarding the $B(E2)$ and $B(M1)$ values, as well as the energy levels, indicates that the NPA provides an appropriate theoretical framework to describe low-lying states of these nuclei. Experimental data are relatively scarce in this region. We therefore believe that our predictions (e.g., $E2$ and $M1$ transition rates, and magnetic dipole moments) are useful for future studies of these nuclei.

ACKNOWLEDGMENTS

This work was supported by the National Natural Science Foundation of China (Grants No. 11145005, No. 11225524, No. 11247241, No. 11305101, and No. 11305151), the 973 Program of China (Grant No. 2013CB834401), and the Shanghai Natural Science Foundation of China (Grant No. 13ZR1419000). C. Qi, R. Liotta, and R. Wyss acknowledge the support of the Swedish Research Council (VR) under Grants No. 621-2010-4723 and No. 621-2012-3805. H. Jiang thanks the Shanghai Key Laboratory of Particle Physics and Cosmology (Grant No. 11DZ2260700) and KTH for financial support. Discussions with B. Cederwall and T. Bäck are gratefully acknowledged.

[1] T. Faestermann, M. Górska, and H. Grawe, Prog. Part. Nucl. Phys. **69**, 85 (2013), and references therein.
[2] G. Guastalla *et al*., Phys. Rev. Lett. **110**, 172501 (2013).
[3] T. Bäck *et al*., Phys. Rev. C **84**, 041306(R) (2011).
[4] M. G. Procter *et al*., Phys. Rev. C **86**, 034308 (2012).
[5] M. G. Procter *et al*., Phys. Lett. B **704**, 118 (2011).
[6] M. G. Procter *et al*., Phys. Rev. C **87**, 014308 (2013).
[7] M. Sandzelius *et al*., Phys. Rev. Lett. **99**, 022501 (2007).
[8] I. G. Darby *et al*., Phys. Rev. Lett. **105**, 162502 (2010).
[9] H. Jiang, Y. Lei, G. J. Fu, Y. M. Zhao, and A. Arima, Phys. Rev. C **86**, 054304 (2012).
[10] C. Qi and Z. X. Xu, Phys. Rev. C **86**, 044323 (2012).
[11] I. O. Morales, P. V. Isacker, and I. Talmi, Phys. Lett. B **703**, 606 (2011).
[12] T. Bäck, C. Qi, B. Cederwall, R. Liotta, F. Ghazi Moradi, A. Johnson, R. Wyss, and R. Wadsworth, Phys. Rev. C **87**, 031306(R) (2013).
[13] S. N. Liddick *et al*., Phys. Rev. Lett. **97**, 082501 (2006).
[14] T. Faestermann, A. Gillitzer, K. Hartel, P. Kienle, and E. Nolte, Phys. Lett. B **137**, 23 (1984).
[15] C. Qi, F. R. Xu, R. J. Liotta, R. Wyss, M. Y. Zhang, C. Asawatangtrakuldee, and D. Hu, Phys. Rev. C **80**, 044326 (2009).
[16] C. Qi, D. S. Delion, R. J. Liotta, and R. Wyss, Phys. Rev. C **85**, 011303 (2012).
[17] http://www.nndc.bnl.gov/ensdf/
[18] B. Hadinia *et al*., Phys. Rev. C **72**, 041303(R) (2005).
[19] O. Möller, N. Warr, J. Jolie, A. Dewald, A. Fitzler, A. Linnemann, K. O. Zell, P. E. Garrett, and S. W. Yates, Phys. Rev. C **71**, 064324 (2005).
[20] G. J. Lane *et al*., Phys. Rev. C **57**, R1022 (1998).
[21] G. de Angelis *et al*., Phys. Lett. B **437**, 236 (1998).
[22] K. Starosta *et al*., Phys. Rev. C **61**, 034308 (2000).
[23] B. Hadinia *et al*., Phys. Rev. C **70**, 064314 (2004).
[24] J. M. Sears, I. Thorslund, D. B. Fossan, P. Vaska, E. S. Paul, K. Hauschild, I. M. Hibbert, R. Wadsworth, and S. M. Mullins, Phys. Rev. C **57**, 1656 (1998).
[25] M. Petri *et al*., Phys. Rev. C **76**, 054301 (2007).
[26] Zs. Dombrádi, Phys. Rev. C **51**, 2394 (1995).
[27] J. Q. Chen, Nucl. Phys. A **626**, 686 (1997); J. Q. Chen and Y. A. Luo, *ibid*. **639**, 615 (1998); Y. M. Zhao, N. Yoshinaga, S. Yamaji, J. Q. Chen, and A. Arima, Phys. Rev. C **62**, 014304 (2000).
[28] H. Jiang, G. J. Fu, Y. M. Zhao, and A. Arima, Phys. Rev. C **84**, 034302 (2011); G. J. Fu, J. J. Shen, Y. M. Zhao, and A. Arima, *ibid*. **87**, 044312 (2013).
[29] Y. A. Luo and J. Q. Chen, Phys. Rev. C **58**, 589 (1998); K. Higashiyama and N. Yoshinaga, *ibid*. **88**, 034315 (2013); L. Y. Jia, H. Zhang, and Y. M. Zhao, *ibid*. **75**, 034307 (2007).
[30] Z. Y. Xu, Y. Lei, Y. M. Zhao, S. W. Xu, Y. X. Xie, and A. Arima, Phys. Rev. C **79**, 054315 (2009).
[31] F. Iachello and A. Arima, *The Interacting Boson Model* (Cambridge University, Cambridge, England, 1987); F. Iachello and I. Talmi, Rev. Mod. Phys. **59**, 339 (1987).
[32] K. Allart, E. Boeker, G. Bonsignori, M. Saroia, and Y. K. Gambhir, Phys. Rep. **169**, 209 (1988).
[33] J. N. Ginocchio, Ann. Phys. (NY) **126**, 234 (1980); C. L. Wu, D. H. Feng, X. G. Chen, J. Q. Chen, and M. Guidry, Phys. Rev. C **36**, 1157 (1987).
[34] A. Banu *et al*., Phys. Rev. C **72**, 061305(R) (2005).
[35] Y. Lei, Z. Y. Xu, Y. M. Zhao, and A. Arima, Phys. Rev. C **80**, 064316 (2009); **82**, 034303 (2010); Y. Lei, Y. M. Zhao, and A. Arima, *ibid*. **84**, 044301 (2011) and references therein.
[36] A. J. Boston *et al*., Phys. Rev. C **61**, 064305 (2000).
[37] Y. M. Zhao, S. Yamaji, N. Yoshinaga, and A. Arima, Phys. Rev. C **62**, 014315 (2000).